MASTERARBEIT | MASTER'S THESIS

Titel | Title

Optimization of the production process of PET nanoparticles as well-defined test materials for in-vitro and in-vivo testing

verfasst von | submitted by

Lejla Ahčić BSc

angestrebter akademischer Grad | in partial fulfilment of the requirements for the degree of

Magistra pharmaciae (Mag. pharm.)

Wien | Vienna, 2024

Studienkennzahl lt. Studienblatt | Degree programme code as it appears on the student record sheet:	UA 066 605
Studienrichtung lt. Studienblatt | Degree programme as it appears on the student record sheet:	Masterstudium Pharmazie
Betreut von | Supervisor:	Univ.-Prof. Dr. Lea Ann Dailey

This master thesis project was performed from August 2022 to January of 2023 at the Division of Pharmaceutical Technology & Biopharmaceutics at the University of Vienna under the supervision of Univ. Prof. Dr. Lea Ann Dailey. This thesis was realized within the “Imptox” project which received funding from the EU’s Horizon 2020 program (grant agreement n. 965173).

Abstract

Plastic pollution has emerged as a growing problem in the past few decades. Due to its high stability and persistency, micro- and nanoplastics (MNPs) have a slow degradation rate and remain in the environment for several decades. The impact of these MNPs on the biosphere and health is not yet fully understood, due to a substantial lack of available reference materials. Subsequently, the development of a standardized production method and comprehensive characterization of model nanoplastics (NPs) particles is required.

In the following thesis, the non-solvent induced phase separation (NIPS) technique was employed to produce polyethylene terephthalate (PET) nanoparticles, since PET belongs to the most used polymers for many different applications worldwide. Ethanol (EtOH, 96%, v/v) was used as a non-solvent, whereas benzyl alcohol acted as a solvent. The following critical parameters were identified, which could potentially alter the particle size distribution (PSD) of the model NPs: i) stirring time, ii) filtration time, iii) centrifugation time, and iv) centrifugation speed. Optimization of NIPS by modifying these parameters was then investigated. Laser diffraction (LD) was employed for the determination of the PSD. After optimization, the batch-to-batch reproducibility was tested by manufacturing five consecutive batches with the final protocol. Mean values of the percentiles D10, D50, and D90 were assessed alongside the relative standard deviation (RSD), yield (%), fraction < 1 µm (%), and uniformity. The thesis focused on producing model PET NPs where 85 % of the particles produced are smaller than 1 µm. Regarding reproducibility, RSDs of up to 15% were tolerated for D10, D50, and D90.

The production of PET NPs in EtOH (D10: 0.076 µm ± 0.0035 µm, D50: 0.172 µm ± 0.0056 µm, D90: 0.655 µm ± 0.3444 µm) and glycerol (D10: 0.075 µm ± 0.0062 µm, D50: 0.172 µm ± 0.015 µm, D90: 0.462 µm ± 0.057 µm) led to a narrow PSD and achieved the overall goal for all percentiles (n=5, mean ± SD). While the RSDs (EtOH/glycerol) of D10 (4.61%/8.30%) and D50 (3.27%/8.80%) could be improved and met the set criterion, the RSDs of the D90 (52.57%/12.40%) were too high. Possible explanations are the formation of aggregates and contamination with dust during the production and

characterization. Therefore, reproducibility needs to be improved and should be further investigated in future studies.

Table of contents

List of abbreviations

BBB	Blood-brain barrier
BPA	Bisphenol A
EtOH	Ethanol (96%, v/v)
GIT	Gastrointestinal tract
MNP	Micro- and nanoplastic
MP	Microplastic
MW	Molecular weight
NIPS	Non-solvent induced phase separation
NP	Nanoplastic
PE	Polyethylene
PET	Polyethylene terephthalate
PP	Polypropylene
POP	Persistent organic pollutant
PSD	Particle size distribution
PS	Polystyrene
PU	Polyurethane
PVC	Poly vinyl chloride
RSD	Relative standard deviation
SD	Standard deviation
WWTP	Wastewater treatment plants

1. Introduction

1.1. Definition of plastics

According to ISO, plastics are defined as materials that consist of a polymer with high molecular weight and can be formed by flow [1]. Expanding this definition, it is important to add that conventional plastic is hardly soluble in water and mainly belongs to the semicrystalline polymers with a melting point (T_M) and a glass transition temperature (T_G). That's why the aggregate state is hard and brittle below the T_G, whereas soft above T_G but below T_M and liquid above T_M [2].

The most commonly used polymers in Europe are polypropylene (PP), polyethylene terephthalate (PET), polyethylene (PE), polyvinyl chloride (PVC), polyurethane (PU), and polystyrene (PS) [3]. As **Figure 1** shows, these plastics can be divided into two groups based on their backbone structure: plastics with a backbone only consisting of carbon atoms and plastics with heteroatoms, such as nitrogen or oxygen [4]. Plastics with a carbon-carbon backbone such as PP and PE are mainly used in packaging and are more likely to enter the environment, due to their short-time use and high production volume [4], [5].

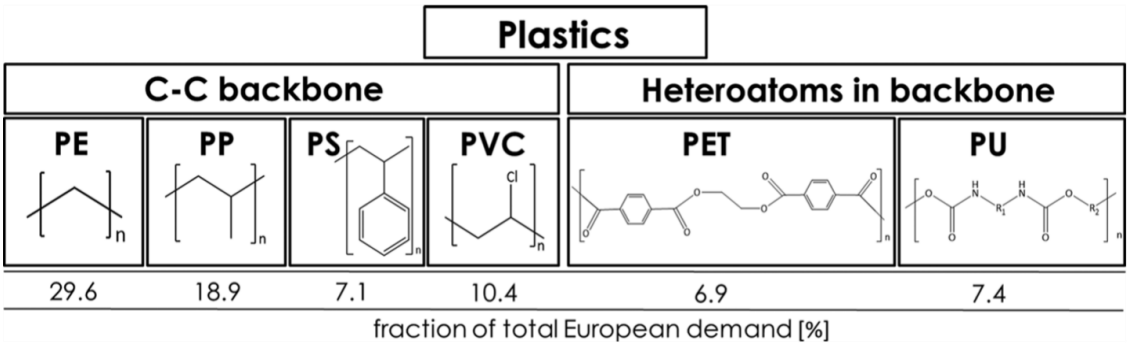

Figure 1: Structures of commonly used plastics in Europe. Reused from Gewert et al. [5] *with permission from the Royal Society of Chemistry.*

Regarding size, there is no standardized international definition. As **Figure 2** shows, there are various definitions from different researchers and institutions. The particles are typically categorized into mega-, macro-, meso-, micro- and nanoplastics (NPs). Macroplastics are commonly defined as plastic particles above 5 mm, whereas mesoplastics usually range from 1-10 mm [2]. According to the National Oceanic and Atmospheric Administration (NOAA), all plastic

particles below 5 mm are defined as microplastics (MPs) [6]. NPs are either defined as particles between 1-100 nm or below 1 µm [2]. In this thesis, the definitions from ISO and the European Union Observatory for Nanomaterials (EUON) were followed, which define NPs as all particles below 1 µm [1], [7], [8].

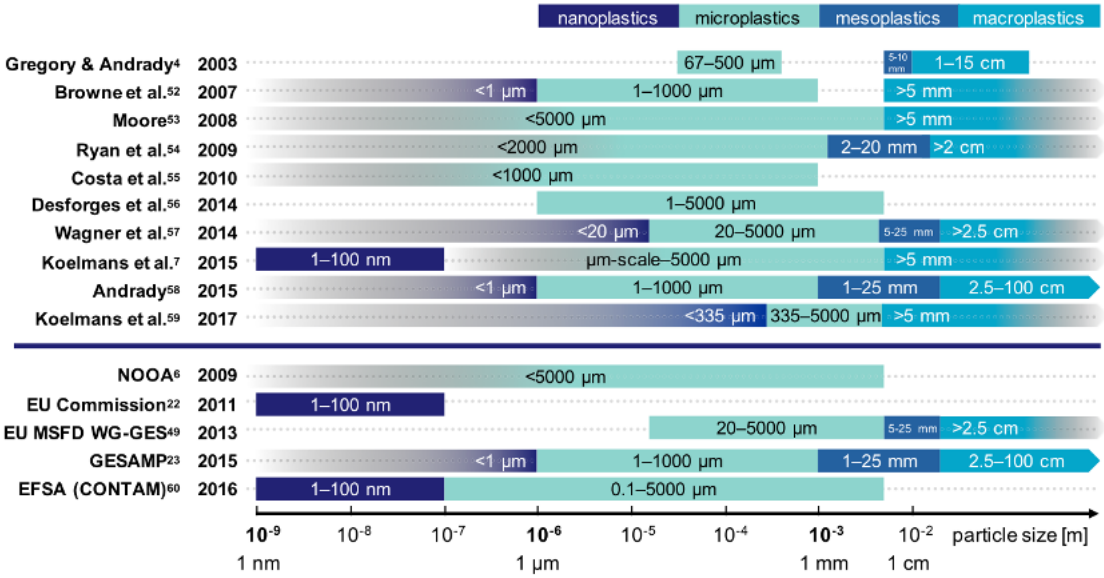

Figure 2: Size categorization from different institutions and research papers. Reused from Hartmann et al. [2] *with permission from the American Chemical Society.*

Furthermore, plastic debris can be classified into primary and secondary plastic. Primary plastic is referred to as plastic produced purposely in a specific size [9], [10]. It can either be manufactured by bottom-up synthetization or by milling larger plastic particles [9]. Secondary plastic on the other hand is generated through fragmentation or degradation from primary plastic [11], [12]. Fragments are usually generated by photochemical or mechanical processes [10]. Primary plastic tends to be more homogenous in terms of shape and size, whereas secondary plastic has an irregular shape with a higher surface area [2]. This favors interaction with its environment [2], [9], [10]. The first approach to degradation happens at the plastic surface. MPs are especially prone to changes due to its high surface-to-volume ratio [5], [13].

1.2. Degradation

Degradation is defined as the breakdown of large objects or fragments into smaller plastic debris [10]. Petroleum-based plastics are the most used and difficult to degrade in the natural environment because of their high molecular weight (MW) and hydrophobic characteristics [13]. Research has shown that

fungal, enzymatic, and photo-oxidative degradation works with petroleum-based plastics. However, further studies under natural conditions are needed to confirm those findings [5], [14]. There are two main pathways of plastic degradation, namely the abiotic and biotic pathways [5].

The abiotic degradation usually takes place first and consists of initiation, propagation, and termination [5]. Initiation can be caused by heat, UV-light, or other mechanisms, where free radicals are produced due to breaking chemical bonds in the backbone of the polymer. It is important to note that photo-initiation can only occur if chromophores are part of the chain. However, PP and PE, which consist of a carbon-only backbone - as mentioned in chapter 1.1 - can still undergo photo-degradation because of impurities in their structure [13]. The environment affects the degradation process as well. It is hypothesized, that micro- and nanoplastics (MNPs) degrade more readily in coastal areas than in groundwater because of UV irradiation [15]. Temperature influences the degradation rate through increased hydrolysis, enzymatic activity, and by changing the molecular mobility of the polymer [13], [16]. Furthermore, the production of free radicals is increased because chemical reactions are accelerated with increasing temperature [16]. Another important factor is humidity, where higher humidity levels lead to faster degradation by enhancing hydrolysis and chain scission [13], [17]. Research by Edge *et al.* [17] showed that the chain scission of PET particles was 5 times higher at 100% relative humidity than at 45% at a constant temperature of 60°C. During the propagation, which marks the next step, previously produced free radicals react with oxygen and form peroxy radicals [13]. This process results in cross-linking and random chain scission in the polymer's structure, where plastic fragments with lower MW emerge. Those fragments have a greater surface area which makes them available for further reactions [4], [5], [18]. Termination of the radical reaction is achieved when inert products occur [19]. Finally, the degraded plastics possess several oxygen-containing functional groups like aldehydes and ketones which makes them more hydrophilic and therefore accessible to biodegradation [4].

Microbes and enzymes play a crucial role in the following biotic pathway, which ideally leads to mineralized particles. Biodegradation mainly consists of the following steps: colonization, biodeterioration, fragmentation, assimilation, and

lastly mineralization [4]. The process starts with colonization, where microbes attach to the surface of the particles, grow, and ultimately form a biofilm [4], [14], [20]. During the biodeterioration, extracellular enzymes like peroxidase, alter the polymer's surface through hydrolytic cleavage [4], [21]. A higher number of strains also contributes to a higher biodeterioration rate. In terms of physical deterioration, some species can infiltrate the surface of the polymer and create pores. Fragmentation enhances the further lysis of the polymers to oligomers, dimers, or monomers by the release of enzymes like hydrolases or oxidoreductases. This stage can take longer because of substrate exhaustion and is the main reason why plastic has long durability in the environment [4]. The next step is the assimilation of the monomers into the microbial cell, where due to differences in cell permeability, not every monomer can enter the cell [4], [20]. The last step of the biotic pathway is the mineralization of the monomers through oxidation. Under aerobic conditions, the monomers are mineralized into CO_2 and H_2O, whereas in an anaerobic environment also CH_4 is produced [4], [5], [20].

The success of degradation also depends on the additives used in plastic production, which are added to modify the material properties. For instance, antioxidants and stabilizers provide a higher resistance against photodegradation and therefore slow down the natural degradation process [5], [13].

1.3. Sources and environmental impact

Plastic debris can nowadays be found everywhere on our planet and beyond. It reaches from the marine and terrestrial areas to the atmosphere [12]. It is estimated that plastic can stay in the environment for hundreds of years and accumulate due to its durability [12], [22]. The most important sources of plastics are land- and sea-based. Due to its characteristics, plastic can move great distances and therefore a large fraction of land-based plastics find their way to the marine environment [15]. In terms of terrestrial plastic debris, they can originate from urban and transport infrastructure, manufacturing, personal care products, and agriculture [15], [23]. MNPs are mostly released through synthetic materials, residues from industrial areas, abrasion from fiber materials or tires, and transportation through dust [15], [24]. It has also been shown that landfills

act as a source of MPs and that the escape of those particles cannot be avoided [25].

MNPs are released into the marine ecosystems via different pathways [22]. They can be released through daily human activities like tourism, aquaculture, shipping, beach littering or fishing [15], [26], [27]. The distribution takes place by rivers, air transport, directly at the seaside, and wastewater treatment plants (WWTP) [15], [26]. A study by Lebreton *et al.* [26] estimated that 1.15 – 2.41 million tons of plastic debris enter the ocean through rivers each year. Therefore, MPs can be found in all major ocean basins, involving the shoreline, seabed, sea surface, and water column [26], [28]. WWTP cannot filter NPs, thus they can enter the sea, groundwater, and ocean, as well [29]. Studies by Kazour *et al.* [30] showed that the distance to the WWTPs has an essential influence on the accumulation of plastic particles. The further the WWTPs outflow from the sampling site, the lower the amount of MPs detected in surface water. It was also found that inner lagoons with a low water movement show a higher accumulation than outer lagoons [30]. Plastic particles were also found in previously untouched places like the Antarctica and Arctic Sea ice [31].

It is hypothesized that MNPs can also be transported through sea salt aerosol and reach coastal areas by wind where airborne MNPs can be inhaled [32], [33]. It is also supposed that the use of wastewater sludge, which can contain NPs, as fertilizer in agriculture can contribute to NPs in the atmosphere due to the wind-driven transport of NPs after the sludge is dried [29], [32]. Indoor air is also a potential source. A study by Dris *et al.* [40] showed that 33% of fibers collected indoors were petrochemical-based [34].

It is important to emphasize, that plastic as a component does not solely contribute to the pollution. Plastic particles also operate as a vector for persistent organic pollutants (POPs) [4]. These include polychlorinated biphenyls (PCB), various pesticides, and polycyclic aromatic hydrocarbons (PAHs) [13], [35]. Due to its hydrophobic surface, plastic debris can adsorb these POPs or accumulate heavy metals such as lead [4]. They can reach environmental concentrations in the ng/g to µg/g range and, when ingested or inhaled, form a potential risk for humans and other organisms [36], [37]. Through WWTPs, residues from agriculture, industries, urban areas, and sewage sludge, plastic debris makes its

way into the groundwater and as well reaches the cycle for human exposition [38].

1.4. Exposure and possible health implications

The exposure of humans to plastic is ubiquitous and there is hardly any part in a human's life that is not under plastic's influence. MNPs can enter the body through ingestion, inhalation, or dermal absorption but are not equally relevant [31]. The main exposure route for humans is oral ingestion because many food products are contaminated with MNPs [10], [31]. They have been found in processed food, beverages, sea salt, plastic teabags, sugar, honey, clothing fibers, and seafood [32]. It is only a matter of time until the majority of the food chain is contaminated with plastic due to its ubiquitous appearance, rising global use, and possible migration of NPs from packaging materials [29], [39]. A study by Cox *et al.* [40] has shown that seafood, bottled water, and inhalation contribute the most to the overall intake. Salt, honey, alcohol, sugar, and tap water, which all contained MPs, were also investigated but added only a fraction to the previously mentioned MPs load. Regarding water, the results showed an average annual intake of 90,000 particles per year when only bottled water was consumed [40].

The gastrointestinal tract (GIT) with its big surface area represents the primary exposure route, as MNPs can be consumed unintentionally through plastic-contaminated products. Mucus represents the first barrier of the GIT [32]. However, it has been shown that nanoparticles can pass the mucosal barrier by pinocytosis and phagocytosis, which is an essential part of the non-specific immune response [31]. Subsequently, they can reach the underlying epithelial cells, specifically the M-cells of the Peyer's patches [41]. Here, the uptake of plastic particles takes place through endocytosis [32], [42]. Another possible route of uptake is paracellular persorption [32], [41], [42]. *In-vitro* studies showed that PS NPs can pass the intestinal barrier. However, these studies were only performed with model NPs and do not represent environmental samples [29].

Another possible route for intake is inhalation. Particles > 1 µm can enter the lung lining fluid which consists of mucus and surfactant. However, they cannot pass

the epithelial barrier because of their size and through mucociliary clearance, those particles eventually end up in the gut [32]. Due to the lung's high surface area, particles < 1 µm can potentially be taken up across the epithelium. Through diffusion or active cellular uptake, NPs enter the capillary blood system with subsequent distribution in the human body [29], [32]. Studies on nylon workers showed that they had several types of plastic residues from production in their lung tissues and showed clinical symptoms of allergic alveolitis [32], [43].

Recent studies by Kopatz *et al.* have shown that NPs can also reach the blood-brain barrier (BBB) and that the composition of the biomolecular corona surrounding the particles impacts the BBB passage. Cholesterol molecules on the corona could improve this passage, whereas a protein corona inhibited it. Also, the size of the NPs played a crucial role in the effectiveness of the BBB: Particles bigger than 0.293 µm could not pass the barrier in this study [44].

Regarding biochemical reactions in organs, NPs are possibly linked to changes in gene expression, transcription factors, oxidative stress, and DNA fragmentation. The accumulation of MPs can lead to cytotoxicity by triggering an immune response, hypersensitivity, and acute reactions [31]. Hwang *et al.* [45] showed a stimulating effect on the immune system and hypersensitivity towards PP particles by increased production of histamine and cytokines of different cell types. Histamine is a pro-inflammatory mediator that plays an essential role in the development of allergies [46]. Its imbalance can implicate the development of different diseases including allergies [45], [47]. However, further studies with different plastic sizes and concentrations are crucial to understanding the mechanisms and effects on humans [45].

In-vivo studies by Chen *et al.* and *in-vitro* studies with human epithelial cells by Cortés *et al.* showed that NPs generated a high amount of reactive oxygen species (ROS) [35], [48]. Including hydrogen peroxide or superoxide, which can damage the cell membrane, DNA, and various proteins. NPs can furthermore induce acute or chronic inflammation, apoptosis, and necrosis [31], [32], [44].

The stratum corneum of the skin forms a protective barrier against environmental influences. Usually, plastic particles cannot pass this barrier. However, there are possible ways how NPs could penetrate the skin like through hair follicles, sweat

glands, or injured skin [29], [49]. In a study by Alvarez-Roman *et al.* PS NPs of 20 nm showed a higher accumulation in the follicular openings than PS NPs of 200 nm in diameter. Neither of the particles were found in deeper skin tissues [50].

Also, effects on marine organisms are known, where MNPs can cause harm and death due to entanglement and ingestion. Furthermore, for some animals like pacific oysters, exposition to NPs can lead to deformation, infertility and a decrease in embryogenesis [31], [15]. PS NPs have also been found to affect the chromosomes by inducing aberrations [31].

In terms of additives or POPs like phthalates or bisphenol A (BPA), plastic debris plays an important role as a carrier for reaching the human body [36]. Research by Koelmans *et al.* showed that additives like BPA and nonylphenol leach from plastic debris ingested by marine organisms [51]. BPA is a highly used antioxidant or plasticizer in various polymers and several studies have shown that BPA can migrate from plastics into food and drinks [15]. POPs and their derivates are considered to be toxic and can induce endocrine disruption, mutagenesis, or carcinogenesis [36]. It is known as an agonist for the estrogen receptors and an antagonist for thyroid hormone action [52]. Moreover, BPA can change the beta cell function in the pancreas and promote obesity and cardiovascular diseases [53]. The full effects on organisms have yet to be fully discovered [54]. Phthalates are used in plastics to convey flexibility and durability and can be potentially harmful to the reproductive system [15], [55]. It has been shown that exposure to phthalates leads to an increased prevalence of allergic respiratory diseases [56]. Research by Bolaji *et al*. showed that Dibutyl phthalate (DBP) can accumulate in lung tissues and worsen the development of asthma [57]. A study by Maestre-Batlle *et al*. on humans concluded that DBP exposure by inhalation led to amplified allergy-caused lung function decline [56].

Plastic particles can not only carry chemicals or metals but can also act as vectors for human pathogenic microbes such as *Escherichia coli* or *Bacillus cereus*. These bacteria can colonize the surface of MPs and lead to the spreading of microbial diseases. Furthermore, antibiotic resistance development could be enhanced when plastic and antibiotic-contaminated water come into contact [58].

To assess the possible risks of NPs, test materials with precisely known characteristics are crucial. Furthermore, it is essential to develop suitable detection methods for *in-vivo* studies and environmental samples. So far, it is very challenging to detect them in the environment due to their small size and low environmental concentrations. Furthermore, the matrix from NPs needs to be removed for proper detection without changing the properties and losing particles [11], [59]. A detailed characterization is vital to get in-depth information on particle size, shape, stability, and toxicity for *in-vivo* studies [11]. Therefore, standardized NPs with a known size, shape, concentration, and well-defined matrix are urgently needed for research purposes [59].

1.5. Production of NP test materials

There are mainly two approaches of producing MNPs: bottom-up and top-down. The bottom-up approach involves polymerization which can be induced by emulsion, dispersion, suspension, or precipitation. On the other hand, top-down means the size reduction of larger plastic particles by milling or ultra-sonic treatment [60].

The method used for this thesis was the nonsolvent-induced phase separation (NIPS), which can neither be assigned to a bottom-up nor a top-down approach. NIPS works by dissolving a polymer in a suitable solvent, followed by mixing the solution with a non-solvent. This leads to nanoprecipitation, which induces the phase separation and recrystallization of the NP particles [61], [62], [63]. Advantages of this method are high yields, simplicity, and time efficiency when compared to commonly used production methods [62]. Another benefit is that no further degradation occurs except during the heating for dissolution, as this could lead to changes in the polymer's structure through enhanced hydrolysis [13], [64].

Nanoprecipitation can be divided into the following parts: supersaturation, nucleation, and growth. Supersaturation occurs when the concentration of the solubilized material is higher than the saturation value during equilibrium [65]. If non-solvent is added, the solvent potency for dissolution decreases and the system achieves the supersaturated state [65]. The higher the supersaturation, the smaller the resulting particle size. Supersaturation generates a high Gibbs

free energy and to reach the next step, the nucleation, the Gibbs energy needs to be reduced. This is caused by the formation of precipitated particles and a maintained equilibrium concentration in the solution [61], [65]. The reduced Gibbs energy is balanced by an increased surface energy [61]. The growth of nuclei continues until the supersaturation decreases under the critical concentration [65]. When the nucleation happens under rapid and uniform conditions, smaller particles with a narrow particle size distribution (PSD) emerge [61]. Besides growth by condensation, which is defined as the addition of individual molecules to the particle surface, it can also occur due to coagulation [65]. The adhesion of particles happens when attractive interactions exceed the repulsive ones and when collision between particles is high. This is the case when the collision efficiency is increased due to faster motion, higher particle concentration, or bigger particle size. Therefore, coagulation needs be avoided when NPs should be produced [65]. Ideally, a high supersaturation with an increased volume of non-solvent and a low polymer concentration with low coagulation should be used to produce small particles [61].

1.6. The IMPTOX project

The IMPTOX project represents the EU's Horizon2020 program that mainly focuses on the possible impacts of MNPs on the development of allergies and consists of a multidisciplinary team in 8 European countries. One of the aims relevant to this thesis is the production and characterization of test materials for the development of new analytical methods and their use in *in-vitro* and *in-vivo* studies [66].

1.7. Aim of the thesis

The main objective of the thesis was to optimize the production method for model PET nanoparticles and their characterization with suitable analytical methods. Methods from Lee *et al.* and Achilias *et al.* were adopted, which produced PP NPs by NIPS and which utilized the dissolution/reprecipitation method to recycle various polymers, respectively [62], [64]. Through optimization of the PET nanoprecipitation process, it was aimed to increase the fraction of particles < 1

µm to at least 85% of the volume-based distribution. Additionally, the reproducibility of the production method was evaluated. The aim was an RSD below 15% of the percentiles D10, D50, and D90 between 5 consecutively produced batches.

2. Materials and methods

2.1. Chemicals and materials

Granules of PET were kindly provided by PlasticsEurope. Nylon membrane filter (0.8 µm, 7408-004) was purchased from Cytiva Whatman (Maidstone, UK). Hydrophilic nylon mesh filter (10 µm, NY1004700) and polycarbonate membrane filter (2 µm, TTTP04700) were obtained from Merck Millipore KGaA (Billerica, USA). Glass filter holders (511-0666) were purchased from VWR International GmbH (Vienna, Austria) and glass cell culture tubes (11.5 mL, round bottom, CLS9944916) were purchased from Pyrex (Corning, USA). Benzyl alcohol (HPLC grade, 108006), and anhydrous glycerol (for synthesis, 8.18709) were sourced from Merck KGaA (Darmstadt, Deutschland). Ethanol (EtOH, 96%, v/v) was purchased from Brenntag Austria GmbH (Vienna, Austria).

2.2. Precipitation

The methods from Lee *et al*. and Achilias *et al*. were adopted with modifications in temperature, the precipitation process, type of non-solvent, and cooling time [62], [64]. PET pellets (260 mg) were transferred into a round bottom flask (100 mL) and dissolved in benzyl alcohol (40 mL). This was achieved by connecting the flask to a reflux condenser and placing it in a silicone oil heating bath at 215°C ± 5°C while stirring at 250 rpm for 45 min. Pre-filtered EtOH as nonsolvent (120 mL, 96%, v/v) was transferred into a beaker and stirred at 250 rpm at room temperature. A glass pipette (10 mL) was used, to add the hot PET solution to the stirred EtOH and obtain precipitated PET nanoparticles. The beaker was subsequently covered with a watch glass and the suspension was stirred for 30 min to allow cooling.

2.3. Filtration and resuspension

The suspension was filtered by vacuum filtration using a 0.8 µm nylon membrane. After the filtration was completed, the pump was disconnected, and the particles were washed five times with pre-filtered EtOH (100 mL). During washing, the PET suspension was stirred with a spatula and gently scraped off the membrane several times to enhance the washing process. Subsequently, the membrane was transferred into a pre-weighed Erlenmeyer flask with pre-filtered EtOH (26 mL), and the flask was sonicated for at least 5 min, followed by a 30 sec vortex. This process was repeated until no more aggregates were visible. The filter was then removed, and the flask was weighed again to determine the total yield of the suspension. A sample was drawn (200 µL) and mixed with a Tween80 solution (200 µL, 5%, w/w) in a glass vial for the size distribution measurement via laser diffraction.

2.4. Size separation

To narrow the particle size distribution, further processing of the obtained PET suspension was necessary. First, the concentration was adjusted to 10 mg/mL by diluting the sample with pre-filtered EtOH. Subsequently, the sample (10 mL) was filtered through a 10 µm nylon mesh. The residues were washed once with pre-filtered EtOH (10 mL). The whole process was repeated for the remaining suspension in 10 mL steps. To receive the final nanoparticle suspension, further separation via centrifugation was performed. The combined filtrate was transferred equally into five glass cell culture tubes (10 mL each) and centrifugated at 493 rcf for 4 min at room temperature using a benchtop centrifuge (Rotanta 460R, Andreas Hettich GmbH & Co. KG, Tuttlingen, Germany) equipped with a swinging bucket rotor (5699-R, radius = 196 mm, max. 5063 rcf). The settings were selected according to a calculation based on Stokes' Law. The sedimentation rate was calculated for particles with a diameter of 2 µm involving the density of EtOH and PET, as well as the viscosity of EtOH. This ensured that particles > 2 µm sedimented and subsequently, mainly nanoparticles remained in the supernatant. The supernatant of each tube was then transferred equally into two clean tubes and filled up with pre-filtered EtOH to 10 mL. The centrifugation was carried out under the same conditions again and the final supernatant and

the remaining pellets of each tube were combined in two separate Erlenmeyer flasks. Samples (200 µL each) of the supernatant and the pellets were prepared for the size distribution measurement as described in chapter 2.6.

2.5. Concentration and yield determination

The concentration was determined gravimetrically by drying an aliquot of the suspension. Therefore, the sample (1 mL) was transferred into a pre-weighed Eppendorf tube (*tare*) and the total weight ($m_{Suspension}$) was noted. The tube with the sample was connected to a rotary evaporator (Rotary Evaporator WB 2001, Heidolph Instrument GmbH & co KG, Schwabach, Germany) and dried at a water bath temperature of 60°C and a pressure of 200 mbar. The pressure was reduced stepwise over one hour until the drying process was completed. Subsequently, the total weight of the dried PET (m_{dried}) was determined.

The concentration was calculated according to **Equation 1**:

Equation 1: Equation for the calculation of the suspension's concentration

$$concentration_{suspension}\left(\frac{mg}{g}\right) = \frac{(m_{dried} - tare)}{(m_{Suspension} - tare)} * 1000$$

To assess the total yield, the total weight of the final suspension ($suspension_{in\ ethanol}$) was gravimetrically determined by using a pre-weighed Erlenmeyer flask. The weight of the starting material ($m_{PET\ pellets}$) was determined at the beginning of the experiments as described in chapter 2.2.

The total yield (%) was calculated via the following **Equation 2**:

Equation 2: Equation for the calculation of the yield in %

$$yield\ (\%) = \frac{suspension_{in\ ethanol}(g) * concentration_{suspension}\left(\frac{mg}{g}\right)}{m_{PET\ pellets}(mg)} * 100$$

2.6. Size distribution measurement

Particle size distribution was determined via laser diffraction (Mastersizer 3000, Malvern Panalytical, United Kingdom). For the measurement, an aliquot of the sample was mixed in a 1:1 ratio with a Tween80 (5%, w/w) solution. The Tween80

solution was prepared with particle-free water and filtered through a polyvinylidene difluoride (PVDF) membrane (0.22 µm) with a syringe.

First, the measurement cell was washed with particle-free water, then filled up with particle-free water and Tween80 (5%, w/w) solution (400 µL) was added before the background was measured. Then, the sample was sonicated and vortexed, and was added in 50 µL increments into the cell until an obscuration level of 3-5% was obtained. Mie theory was used as scattering model, which required the refractive indices of water (1.331), PET (1.636), and the particle absorption value (0.010). The suspension was stirred at 1000 rpm and an average particle size distribution (PSD) of 10 repeated measurements was calculated. Finally, the D10, D50, and D90 values, representing the 10^{th}, 50^{th}, and 90^{th} percentiles, were used to describe the PSD. Another parameter is the uniformity value, which describes the spread of the distribution. A low uniformity value is equivalent to a narrow size distribution. Finally, relative standard deviations (RSDs) of all three percentiles were calculated to assess reproducibility.

2.7. Medium exchange to glycerol

Glycerol was heated in a water bath at 70°C and the PET suspension was transferred into a pre-weighed round bottom flask and subsequently, the weight of the suspension ($susp_{EtOH}$) was determined. The concentration (c_{susp}) was assessed as described in chapter 2.5. The amount of glycerol was calculated using the following **Equation 3**:

Equation 3: Equation for the calculation of the mass of glycerol needed in g to obtain a 40 mg/g suspension

$$glycerol\ (g) = \frac{susp_{EtOH}(g) * c_{susp}(\frac{mg}{g})}{c_{final}(\frac{mg}{g})}$$

A concentration (c_{final}) of 40 mg PET nanoparticles per gram glycerol was defined as the standard. After sonicating the suspension for 5 min, the calculated amount of hot glycerol was added to the PET mixture and immediately vortexed. Subsequent sonication (1 min) ensured an evenly distributed sample. The total

weight of the flask was noted, and the flask was connected to a rotary evaporator (Rotary Evaporator WB 2001, Heidolph Instrument GmbH & co KG, Schwabach, Germany). The water bath temperature was set to 40°C and the pressure was set to 400 mbar. Over 30 min, the pressure was reduced stepwise to avoid boiling. The flask was then weighed every 15 min, to determine the weight loss. The process was considered completed if the weight loss was less than 1%.

2.8. Statistical analysis

Statistical analysis was performed with Microsoft® Excel for Mac (Version 16.83). Statistical significance was considered at a p-value <0.005.

3. Results and discussion

3.1. Assessment of critical parameters

For the entire process of particle formation, there are several parameters that could possibly influence the PSD (**Figure 3**). According to Martinez *et al.* [65] and Hamdallah *et al*. [61], these parameters - dissolution temperature and time, solvent/non-solvent ratio, stirring time and the ethanol addition rate - affect characteristics such as size and surface morphology of the produced NPs. In terms of dissolution temperature, it was shown that a dissolution temperature near the boiling temperature of the solvent decreased the size of the produced nanoparticles [61], [65], [67]. For this reason, a dissolution temperature of 215°C ± 5°C for PET (boiling point benzyl alcohol: 205°C) was chosen.

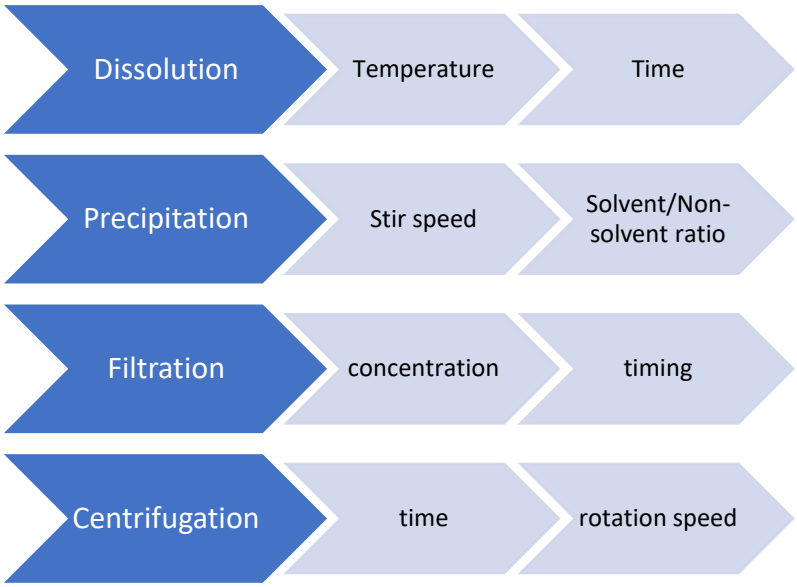

Figure 3: Parameters with possible impact on particle size distribution of nanoparticles

Stirring has an essential influence on the production of nanoparticles. To ensure a narrow PSD it is crucial to stir uniformly and efficient [61], [65]. Filtration as a first approach to size separation, is feasible for removing a large fraction of unwanted larger particles. For fine tuning the PSD, centrifugation with respect to Stoke's Law is possible.

For this thesis, following critical parameters were assessed prior to the beginning of the experiments: stirring time, filtration method, centrifugation time and rotation speed. It was hypothesized that optimization of these parameters can

successfully produce nanoparticles aiming at least 85% for particles of fraction < 1 µm. As for batch-to-batch reproducibility, percentile values D10, D50 and D90 with an RSD below 15 % were intended, respectively.

3.2. Optimization of critical parameters for PET nanoparticle production

3.2.1. Stirring time

To evaluate the influence of the stirring time, the precipitation was carried out under two different conditions. It was hypothesized that the stirring time can influence the particle size while generating smaller particles in comparison to no stirring at all. Firstly, the standard method was used (PET_{std}) with stirring at 250 rpm, and a cooling time of 30 min after precipitation at room temperature. Secondly, the protocol was modified (PET_{mod}) to cool the non-solvent during precipitation with an ice bath and no stirring after precipitation. In this case, the precipitate was filtered directly.

The PSD curves (**Figure 4**) and D-values (**Table 1**) of the standard and modified batch show that the stirring time strongly influences the obtained PSD. The PSD for the standard batch PET_{std} showed the highest peak for particles < 1 µm whereas PET_{mod} had the highest peak for particles > 1 µm. Therefore, it was shown that stirring helps producing smaller particles whereas the removal of stirring generates larger particles. Therefore, PET_{mod} was not considered relevant for the production of nanoparticles. However, the method for PET_{mod} could be used as a basis for production of particles of range 1 – 10 µm in further studies.

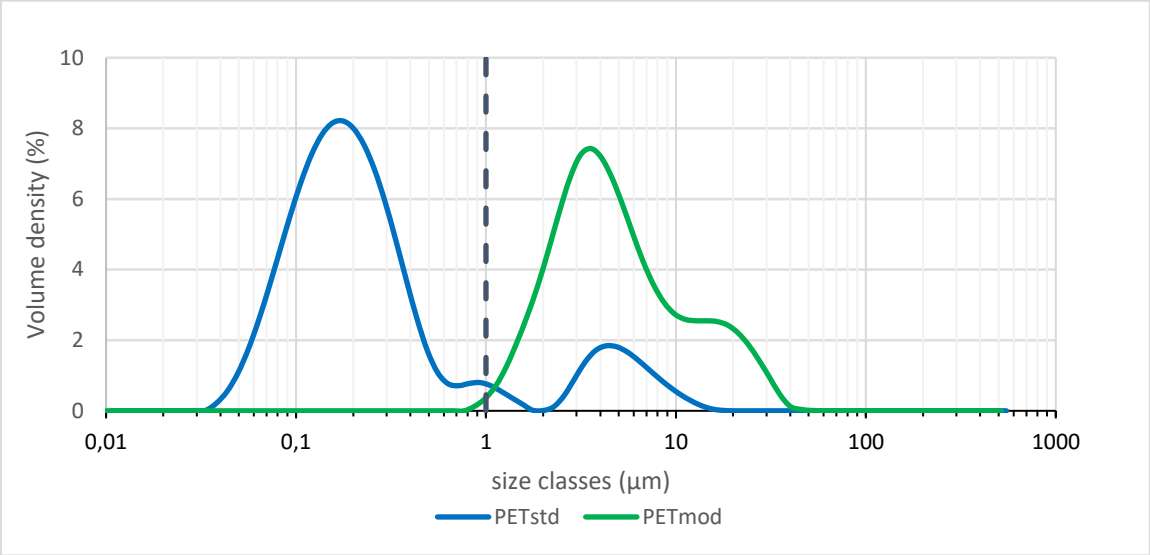

Figure 4: Particle size distribution (PSD) curves of the samples PET_{std} (blue) and PET_{mod} (green). The standard protocol mainly produces particles below 1 µm, whereas the modified protocol shows a substantial shift of the PSD curve above this desired value

As seen in **Table 1**, the percentile values of the PET_{mod} confirmed the results of the PSD as they were above 1 µm and therefore did not reach the goal for producing particles below 1 µm. On the other hand, PET_{std} showed a good basis for nanoparticle production with a D10 and D50 < 1 µm, and was therefore used in the following experiments.

Table 1: Percentile values (D10, D50, D90) from samples PET_{std} and PET_{mod}

Sample	D10 (µm)	D50 (µm)	D90 (µm)
PET_{std}	0.0824	0.195	3.62
PET_{mod}	2.08	4.66	18.2

3.2.2. Filtration after precipitation

To assess the filtration efficiency, the PSD of one batch was measured before and after filtration. It was hypothesized that filtration would exclude particles close to the pore size of the filter used. **Figure 5** shows the PSD directly after the precipitation (PET_01) compared to the PSD (PET_01_filtered) after the filtration. Without filtration, the PSD of PET_01 showed a major peak below 1 µm and several peaks up to the 300 µm range for particles above 1 µm. After filtering this batch through a 10 µm nylon mesh filter (PET_01_filtered), a major peak for particles below 1 µm could be seen alongside a second peak for particles in range 1 – 10 µm. When comparing the two PSD curves, PET_01_filtered shows a smaller peak for particles > 10 µm than PET_01. For particles 1 – 10 µm however, PET_01_filtered revealed an increased peak height compared to PET_01. Therefore, the PSD was only partly improved but did not reach the overall desired PSD for nanoparticles. However, it is important to note that a 10 µm filter was used so the sole purpose for removing particles > 10 µm was achieved with the filtration.

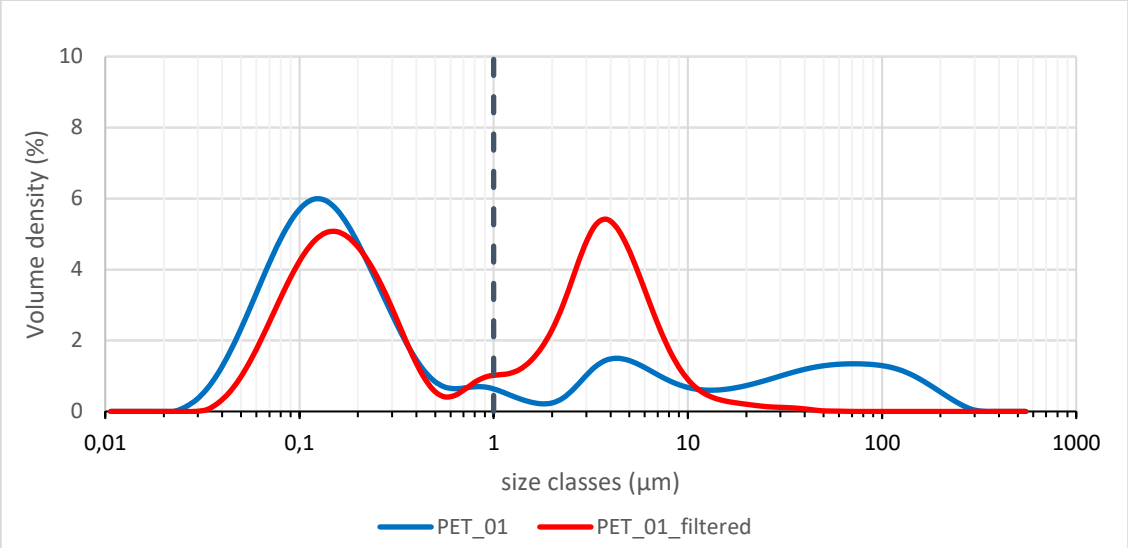

Figure 5: Particle size distribution (PSD) curves of the samples PET_01 (blue) and PET_01_filtered (red). PET_01 shows the PSD directly after precipitation, whereas PET_01_filtered shows the PSD of the same batch after filtration.

When comparing the percentile values, as presented in **Table 2**, PET_01 without filtration showed a high D90 (57.7 µm) which was drastically reduced by filtration

(5.79 µm). Comparing these two batches, it can be concluded that filtration excluded particles larger than the pore size of the filter (10 µm).

Table 2: Percentile values (D10, D50, D90) and fraction < 1 µm (%) from the samples PET_01 after precipitation and PET_01_filtered after filtration

Sample	D10 (µm)	D50 (µm)	D90 (µm)	< 1 µm (%)
PET_01	0.0662	0.208	57.7	80.7
PET_01_filtered	0.0898	0.463	5.79	63.9

When comparing the fraction < 1 µm between PET_01 and PET_01_filtered (**Table 2**), it was shown that PET_01 had a higher total percentage of particles < 1 µm (80.7%) whereas after the filtration PET_01_filtered showed a lower value (63.9%). This could be explained by the fact that NPs get withdrawn by the filter due to aggregation.

To conclude, filtration achieved a cut-off at 10 µm but the overall goal for the production of nanoparticles failed, as the D90 values were above 1 µm. Hence, further steps (centrifugation) were implemented.

3.2.3. Centrifugation

It was hypothesized that the PSD could be narrowed down further by applying centrifugation. Stoke's Law was used to calculate centrifugation speed and time needed to remove particles > 2 µm.

The settings used during centrifugation were modified over three trials. The first sample PET_01 was centrifugated at 140 rcf for 2 min. As shown in **Table 3**, PET_01 showed a low D10 value whereas D50 and D90 were above 1 µm. The PSD of PET_01 shows two major peaks, a smaller one below 1 µm and a larger one above 1 µm, which does not represent the desired PSD. The process was then optimized by modifying the centrifugation speed to 493 rcf while keeping the time unchanged. Furthermore, an additional cycle with the same settings was added (PET_02). As shown in **Figure 6**, the peak height for particles < 1 µm of PET_02 increased and all percentiles were successfully reduced (**Table 3**). It was concluded that the additional cycle and modified centrifugation speed improved the PSD drastically. However, a small peak above 1 µm still remained and subsequently, the centrifugation time was increased to 4 min (PET_03). This led

to a PSD with no substantial contribution of particles > 1 µm. D50 and D90 both decreased compared to PET_02, as seen in **Table 3**.

Table 3: Percentile values of samples PET_01 – PET_03 during optimization of centrifugation (PET_01 represents the standard protocol, PET_02 the first optimized version and PET_03 the final optimized batch)

Sample	D10 (µm)	D50 (µm)	D90 (µm)
PET_01	0.151	2.99	6.47
PET_02	0.0718	0.165	0.541
PET_03	0.0663	0.144	0.33

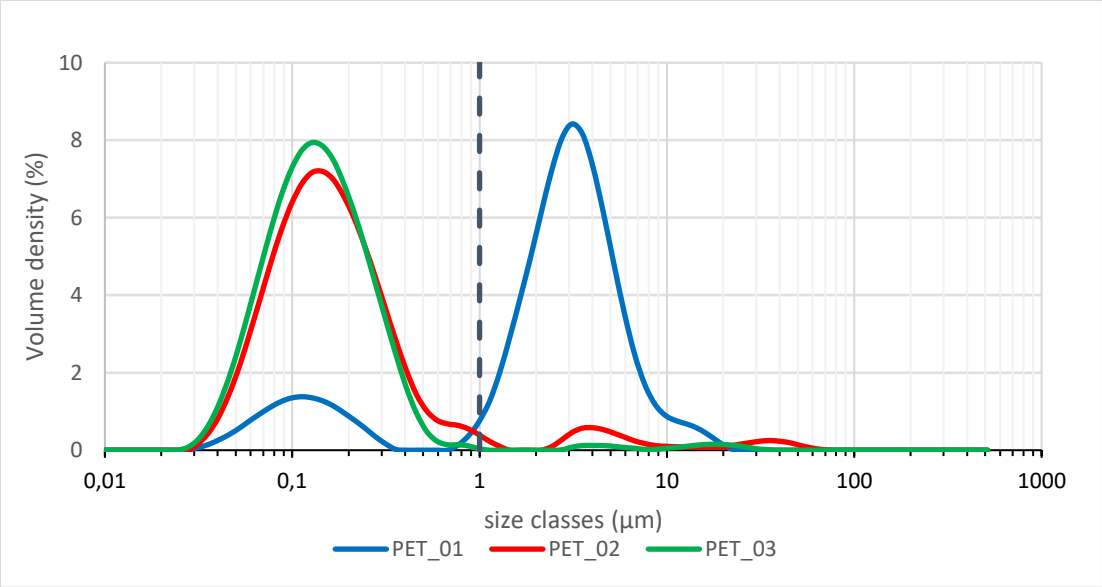

Figure 6: Particle size distribution (PSD) curves of samples PET_01 - PET_03 during optimization of centrifugation. PET_01 (blue) represents the standard protocol, PET_02 (red) the first optimized version and PET_03 (green) represents the final optimized batch.

With the implementation of a centrifugation step, it was possible to achieve the desired PSD. The fraction < 1 µm from PET_02 was further increased for PET_03 from 93.8% to 98.2%, respectively. Ultimately, the goal for fraction < 1 µm was met through implementation and optimization of centrifugation.

3.2.4. Filtration after centrifugation

Aiming for the perfect PSD, it was hypothesized that filtration after completed centrifugation with a nylon mesh filter (2 µm) could remove almost all particles above 1 µm. The PSD of PET_04 showed two major peaks for particles below and above 1 µm after carrying out the additional filtration which, compared to

PET_03 marked a regression rather than an improvement (**Figure 7**). This could be traced back to possible aggregation or contamination during the filtration.

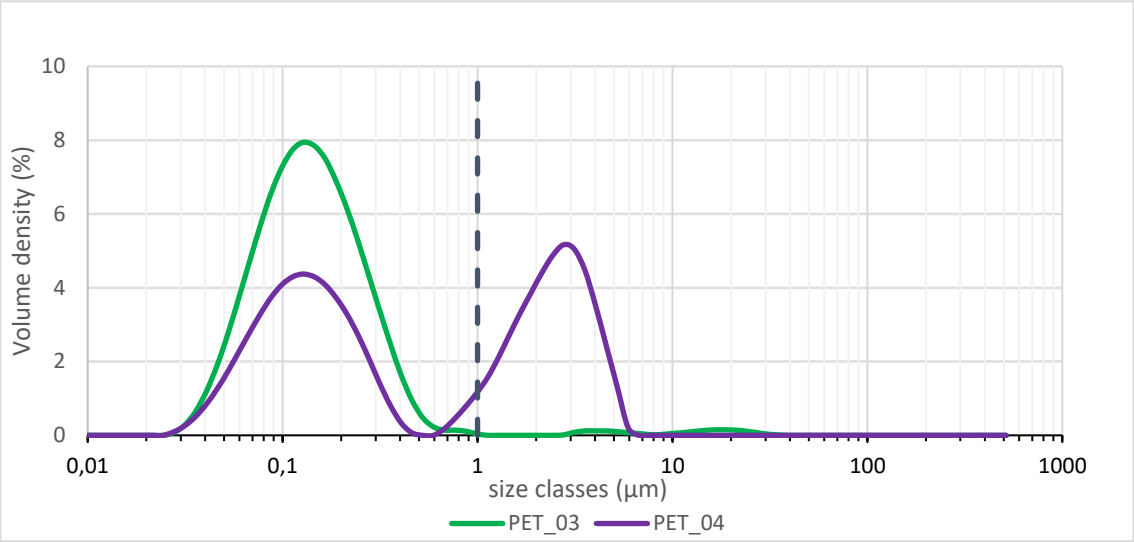

Figure 7: Particle size distribution (PSD) curves of samples PET_03 (green) and PET_04 (violet). PET_03 represents the final batch after centrifugation whereas PET_04 shows the batch of the filtration after centrifugation.

It was concluded that this method failed to achieve the desired removal of particles above 1 µm and that filtration before centrifugation was the better option to improve the PSD as shown in chapter 3.2.3.

3.2.5. Summary

The optimization process is summarized in **Figure 8** by the PSD curves of PET_{std} (directly after precipitation), PET_{centr} (unmodified standard centrifugation protocol, **Figure 8A**), $PET_{optimized\ centr}$ (first optimization of centrifugation, **Figure 8B**) and PET_{final} (final optimization of centrifugation, **Figure 8C**), respectively. Through the optimization efforts, the PSD for nanoparticles could be greatly improved and the goal to produce particles < 1 µm was achieved. The overall PSD was narrowed, the D90 value was reduced down to 0.33 µm (**Figure 9A**) and the fraction < 1 µm was increased to 98.2% (**Figure 9B**) for PET_{final}.

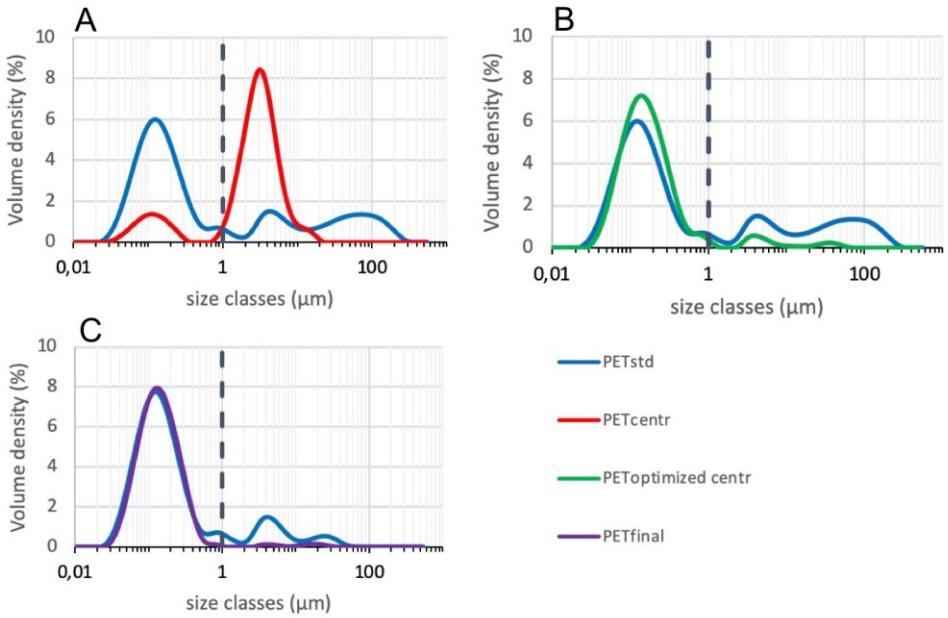

Figure 8: Particle size distribution (PSD) curves representing changes during the optimization process. PET_{std} (blue) represents the batch directly after precipitation, PET_{centr} (red) the unmodified standard protocol for centrifugation, $PET_{optimized\ centr}$ (green) the first optimization of the centrifugation and PET_{final} (purple) the final optimization of the centrifugation.

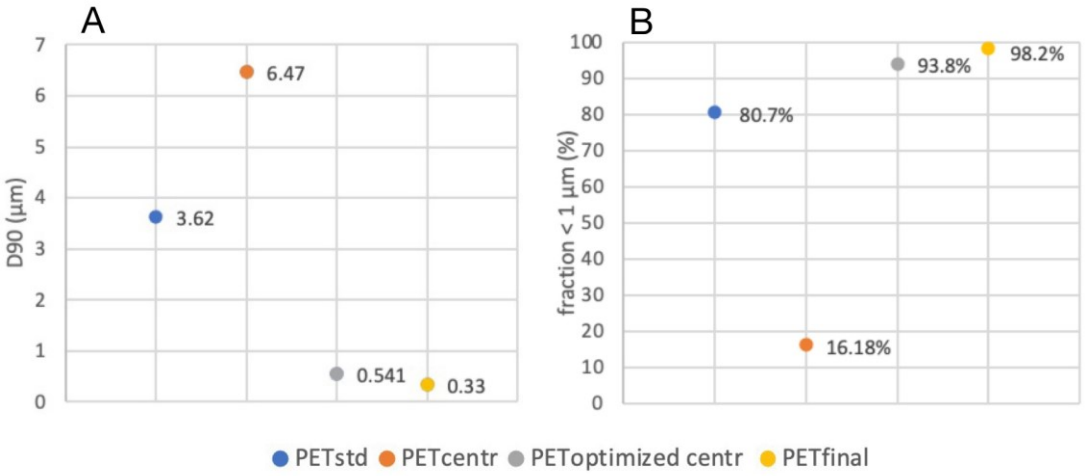

Figure 9: D90 values in µm (A) and fraction < 1 µm in % (B). PET_{std} (blue) represents the batch directly after precipitation, PET_{centr} (orange) the unmodified standard protocol for centrifugation, $PET_{optimized\ centr}$ (grey) the first optimization of the centrifugation and PET_{final} (yellow) the final optimization of the centrifugation.

3.3. Batch-to-batch reproducibility

After the production protocol was successfully optimized, five representative batches out of ten batches produced were chosen to assess reproducibility. Not all batches were comparable, due to changes of the production method.

3.3.1. In ethanol (after production)

From each batch, the following data was assessed: the PSD, D10, D50 and D90, uniformity, yield (%), and the fraction < 1 µm (%). When comparing the PSD curves of PET_A to PET_E (**Figure 10**), PET_A, B and E showed no relevant difference, whereas PET_C and PET_D had a comparable but noticeable different PSD. The peak of PET_C and PET_D at < 1 µm was lower than those of the other samples, which is also reflected in the lower total percentage of the fraction < 1 µm (PET_C: 89.42%, PET_D: 91.91%) than for the other three samples (PET_A: 98.81%, PET_B: 99.00%, PET_E: 99.91%). It is important to note that all samples nevertheless achieved the goal for fraction < 1 µm (>85%).

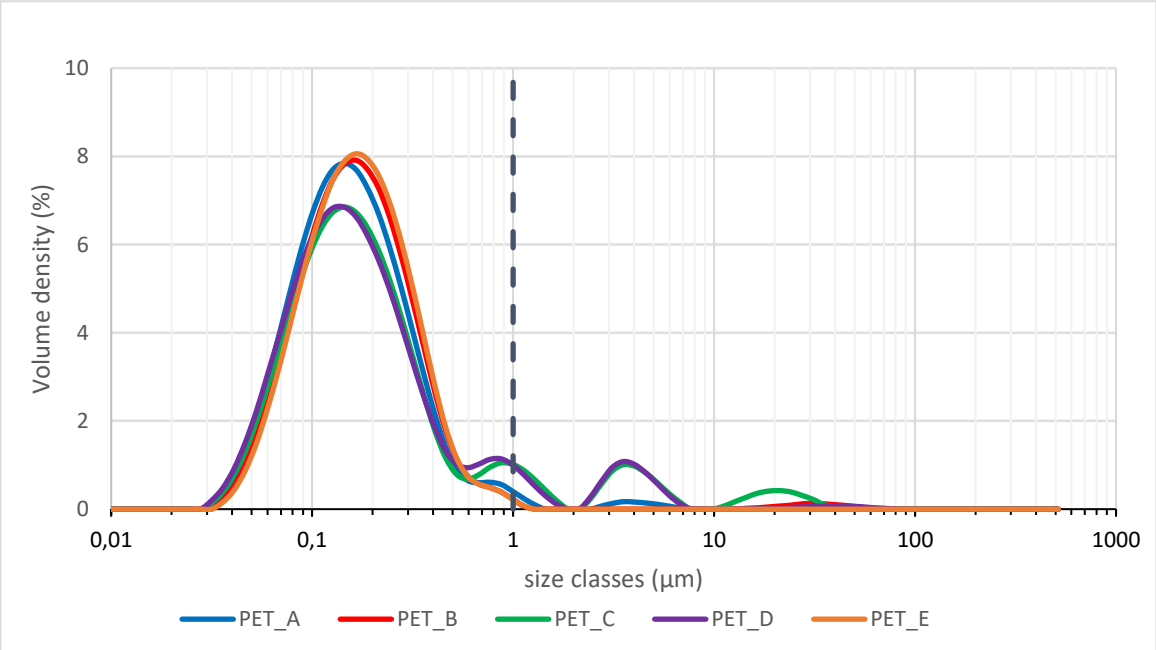

Figure 10: Particle size distribution (PSD) curves from samples PET_A (blue), PET_B (red), PET_C (green), PET_D (violet), PET_E (orange) in ethanol after production (n=5)

Particles > 1 µm could not be excluded in every batch but the contribution to the overall PSD is neglectable. Also, laser diffraction is more sensitive to larger particles as the intensity of scattered light decreases with decreasing particle size. Subsequently, this phenomenon can also lead to overestimation especially when converted to number-based distributions [68]. Fibers from dust could be another reason for peaks > 1 µm, since all experiments were conducted under ambient air. The batches PET_B and PET_E show the smallest peaks for particles > 1 µm and, as expected, the highest total percentage of the fraction < 1 µm (PET_B: 99.00%, PET_E: 99.91%).

Regarding the percentile values, **Figure 11** shows D10, D50 and D90 alongside the mean values (µm) and RSDs (%), respectively. D10 (**Figure 11A**) and D50 (**Figure 11B**) show good reproducibility with mean values < 1 µm and a low RSD whereas D90 (**Figure 11C**) does not met the set criteria (< 15%), as individual values exceeded 1 µm and subsequently increased the RSD to 52.57%. This could be explained by the fact that also the measurement did not occur under optimal conditions and therefore pollutant particles could have been part of the measurement. The Tween80 (5%, w/w) solution used for the measurement could also be investigated. Dust particles could have influenced the PSD measurement. Subsequently, it would be optimal to produce fresh Tween80 solution for each measurement cycle.

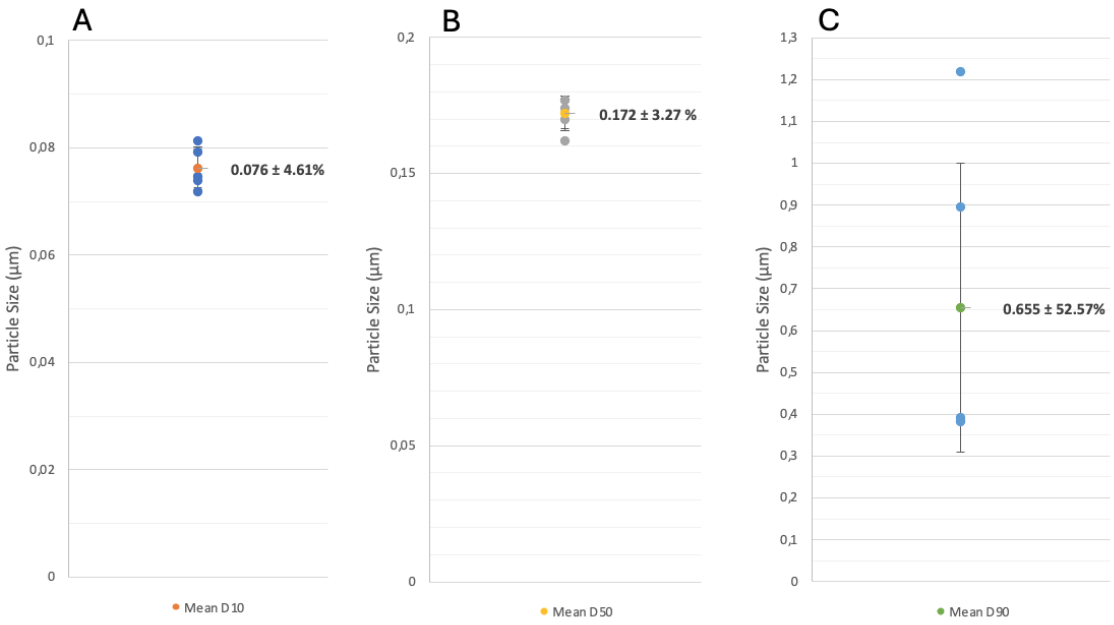

Figure 11: Reproducibility data of batches PET_A-E (n=5). Means of the percentiles D10 (A), D50 (B), and D90 (C) are presented in µm ± RSD in %

Uniformity data shows a low mean value of 2.59 (**Figure 12A**). A low value for uniformity correlates with a narrow PSD. However, it has a high RSD of 71.18%. This could be due to the reasons mentioned before and therefore the consistency of measurements should be improved in further studies. PET_A and PET_D show similar values (PET_A: 0.849, PET_B: 2.448, PET_C: 5.578, PET_D: 3.498, PET_E: 0.556) and out of the 5 samples the lowest ones and had a high total percentage of fraction < 1 µm (PET_A: 98.81%, PET_D: 99.91%).

As shown in **Figure 12B**, the mean yield is relatively high when including the fact that a part of the nanoparticles is lost in the whole process due to filtration and centrifugation. However, the RSD is high (39.26%) and therefore, consistency needs to be improved. The yields for PET_C and PET_E were similar (PET_ C: 42.44%, PET_E: 41.88%), whereas the remaining samples had comparable but low yields (PET_A: 16.92%, PET_B: 19.76%, PET_D: 21.81%). There was no relation found between these similarities.

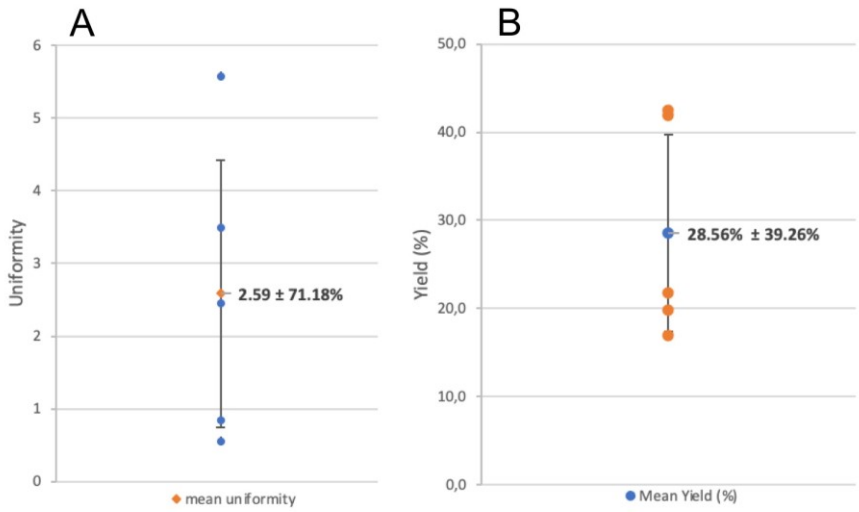

Figure 12: Reproducibility data from PET_A-PET_E (n=5): uniformity (A) and yield (B) including mean values ± RSD in %

3.3.2. In glycerol (final product)

The final product was obtained and evaluated after exchanging the medium to glycerol, which is crucial for the use in cell culture experiments. To obtain enough material, two batches were combined and finally three batches were used for the reproducibility analysis (**Figure 13**). The PSD showed high similarity and is comparable to the ethanolic samples. Particles > 1 µm could not be fully removed and are subsequently part of the final product. Because of the high viscosity of glycerol, colloidal stability is provided, and nanoparticles are prevented from irreversible aggregation. Regarding the fraction < 1 µm, the batches showed similar values, and all achieved the goal of > 85% (PET_F: 94.68%, PET_G: 96.07%, PET_H: 94.29%).

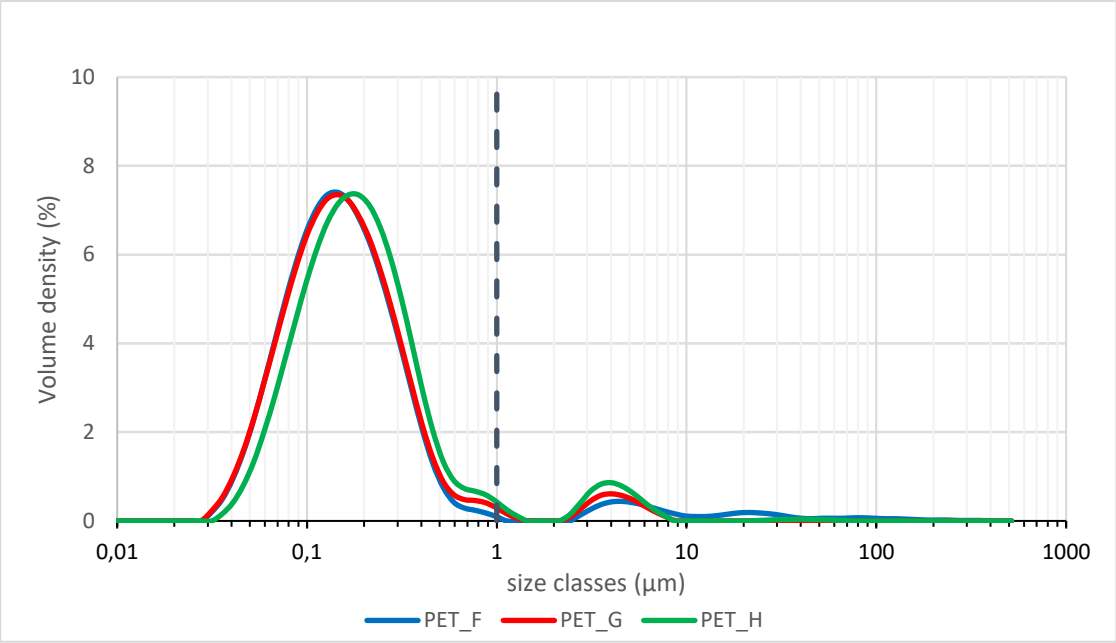

Figure 13: Particle size distribution (PSD) curves of the glycerol samples PET_F (blue), PET_G (red), PET_H (green), n=3

Figure 14A shows the mean percentile values of the samples PET_F to H. All percentiles were < 1 µm and thus, reached the set goal. All percentiles have a low RSD and although D90 was higher than the other two it was below our specified value of <15%. Regarding the uniformity (**Figure 14B**), the mean value and RSD was higher for the glycerol samples (mean: 4.15 ± 76.46%) than for the ethanol samples (mean: 2.59 ± 71.18%). This might be due to the smaller number of replicates or contaminated Tween80 solution when measuring as mentioned in the chapter 3.3.1.

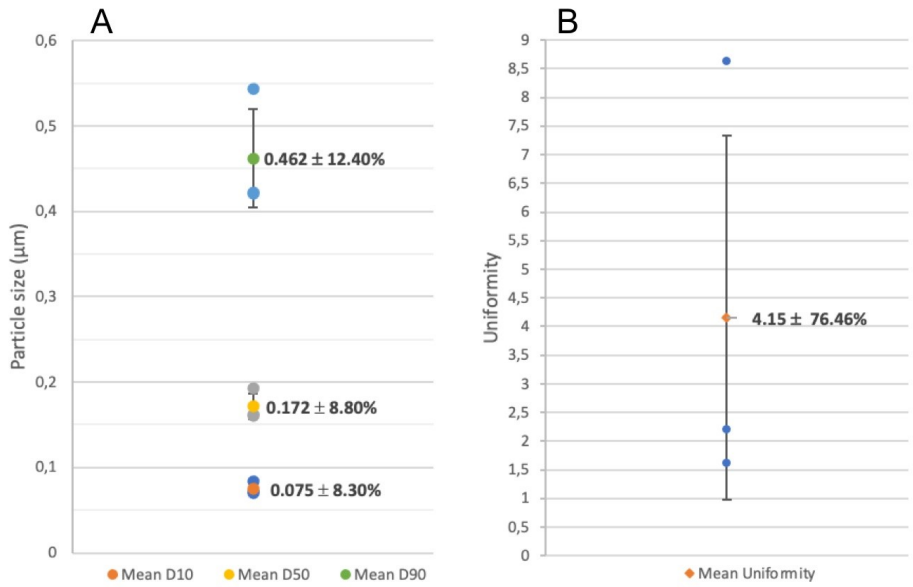

Figure 14: Reproducibility data of PET_F to PET_H. Percentiles D10, D50, D90 in µm (A) and uniformity (B) including mean values ± RSD in % (n=3)

4. Conclusion

It can be concluded that PET nanoparticles can be successfully produced by employing the NIPS technique. The modification and optimization of the investigated parameters - stirring time, filtration, and centrifugation time and speed - resulted in narrowing the PSD, a reduction of all three D-values, and an increase of the fraction < 1 µm.

Stirring time was modified during precipitation whereas the other parameters were altered stepwise after precipitation. A stirring time of 30 min resulted in the production of more nanoparticles and a narrower PSD. In contrast, the use of an ice bath and reduction of stirring time led to particles > 1 µm, which was not desired. The filtration before centrifugation excluded particles > 10 µm and subsequently contributed to the reduction of the PSD range. To remove particles > 1 µm, centrifugation was implemented. By increasing the centrifugation time to 4 min, changing the speed to 493 rcf and implementing a second centrifugation cycle, a better PSD was achieved. Filtration after centrifugation led to worsening the PSD and the introduction of particles > 1 µm. Therefore, this step was not implemented ultimately.

The goal of the fraction < 1 µm being at least 85% was accomplished after optimizing the process. This was achieved for every batch in ethanol (mean

fraction < 1 µm: 95.81% ± 4.48%) and glycerol (mean fraction < 1 µm: 95.01% ± 0.80%). Comparing the RSD values for the percentiles D10, D50, and D90 between the product in ethanol and the final product in glycerol, it is notable that D10 and D50 have a low RSD for both products whereas the RSD for D90 is higher in both cases. The goal of keeping RSDs below 15% was achieved for D10 and D50 of the product in ethanol and glycerol. The RSD of the D90 value of the product in ethanol was above 15% and subsequently failed to meet the set specification. This could be due to fibers from dust or possible contaminants from the Tween80 solution. Another reason could be the higher sensitivity of the measurement technique for larger particles due to higher scattering intensity of those larger particles [68]. However, the RSD of the D90 in the final glycerol product achieved the goal which could be explained by the characteristics of glycerol preventing aggregation.

Ethanol as dispersion medium showed advantages during the production process. NPs were fully resuspendable, the suspension was easy to handle, and it acted as a preservative preventing microbial growth. The final product in glycerol represents a good storage medium because it prevents the nanoparticles from aggregating.

Looking at the yield of the product, there is still room for improvement. A yield of around 30% is seen as mediocre. The RSD of the yield with around 40% represents high variability and should therefore be improved.

Lastly, it should be mentioned that NIPS produces spherical particles in contrast to other methods. Particles with irregular shapes would reflect the plastic fragments in the environment better [60]. However, NIPS outperforms other production methods because of its simplicity, high yield, and time efficiency [62].

5. Outlook

Based on these findings, improving the yield and reproducibility of the PET nanoparticle production should be considered. To achieve this, modifying other parameters like dissolution time and temperature or decreasing the temperature during precipitation should be further investigated [61], [65]. Another crucial factor

during precipitation is the solvent/non-solvent ratio. By increasing the volume of the anti-solvent, the concentration of plastic particles overall is reduced and therefore, aggregation of nanoparticles is less likely to happen. This leads to the formation of more and smaller NPs [61].

The use of surfactants like Tween in the dispersion medium could help to prevent aggregation and therefore promote removing unwanted particles > 1 µm. However, comparability with cell culture should be considered when using surfactants. To improve D90, measurement with freshly prepared Tween80 solution should be investigated. Possible aggregation of particles could also be a reason and improving the sample preparation before PSD measurements should be considered.

For biodistribution tests, fluorescently labeled PET nanoparticles could be produced to offer better detection and tracking. The label should be incorporated in the first step, the precipitation before the dissolution begins. A dye soluble in the used solvent, in this case benzyl alcohol, is therefore required.

Furthermore, stability should be investigated for the products in ethanol and glycerol. This is especially important for possible long-term studies.

List of figures

List of tables

References

[1] International Organization for Standardization, 'ISO/TR 21960:2020(en) Plastics — Environmental aspects — State of knowledge and methodologies'. Accessed: Jun. 11, 2024. [Online]. Available: https://www.iso.org/obp/ui/#iso:std:iso:tr:21960:ed-1:v1:en:term:3.13

[2] N. B. Hartmann *et al.*, 'Are We Speaking the Same Language? Recommendations for a Definition and Categorization Framework for Plastic Debris', *Environ Sci Technol*, vol. 53, no. 3, pp. 1039–1047, Feb. 2019, doi: 10.1021/acs.est.8b05297.

[3] PlasticsEurope, 'An analysis of European plastics production, demand and waste data', 2014. Accessed: Jun. 13, 2024. [Online]. Available:

https://plasticseurope.org/de/wp-content/uploads/sites/3/2021/11/2014-Plastics-the-facts.pdf

[4] S. S. Ali *et al.*, ‘Degradation of conventional plastic wastes in the environment: A review on current status of knowledge and future perspectives of disposal’, Jun. 01, 2021, *Elsevier B.V.* doi: 10.1016/j.scitotenv.2020.144719.

[5] B. Gewert, M. M. Plassmann, and M. Macleod, ‘Pathways for degradation of plastic polymers floating in the marine environment’, Sep. 01, 2015, *Royal Society of Chemistry*. doi: 10.1039/c5em00207a.

[6] Courtney Arthur, Joel Baker, and Holly Bamford, ‘Proceedings of the International Research Workshop on the Occurrence, Effects, and Fate of Microplastic Marine Debris’, 2009. [Online]. Available: www.MarineDebris.noaa.gov

[7] N. P. Ivleva, S. Primpke, and J. M. Lynch, ‘Advances in chemical analysis of micro- and nanoplastics’, Jun. 01, 2023, *Springer Science and Business Media Deutschland GmbH*. doi: 10.1007/s00216-023-04747-y.

[8] A. Kokalj and D. Kühnel, ‘Are nanoplastics hazardous? The way forward to overcome the uncertainties of risk assessment’. Accessed: May 28, 2024. [Online]. Available: https://euon.echa.europa.eu/nanopinion/-/blogs/are-nanoplastics-hazardous-the-way-forward-to-overcome-the-uncertainties-of-risk-assessment

[9] A. J. Kokalj, N. B. Hartmann, D. Drobne, A. Potthoff, and D. Kühnel, ‘Quality of nanoplastics and microplastics ecotoxicity studies: Refining quality criteria for nanomaterial studies’, *J Hazard Mater*, vol. 415, Aug. 2021, doi: 10.1016/j.jhazmat.2021.125751.

[10] M. Bergmann, L. Gutow, and M. Klages, ‘Marine Anthropogenic Litter’, 2015.

[11] T. Hüffer, A. Praetorius, S. Wagner, F. Von Der Kammer, and T. Hofmann, ‘Microplastic Exposure Assessment in Aquatic Environments: Learning from Similarities and Differences to Engineered Nanoparticles’, *Environ Sci Technol*, vol. 51, no. 5, pp. 2499–2507, Mar. 2017, doi: 10.1021/acs.est.6b04054.

[12] J. Brahney, M. Hallerud, E. Heim, M. Hahnenberger, and S. Sukumaran, ‘Plastic rain in protected areas of the United States’, 2020. [Online]. Available: https://www.science.org

[13] A. Chamas *et al.*, ‘Degradation Rates of Plastics in the Environment’, *ACS Sustain Chem Eng*, vol. 8, no. 9, pp. 3494–3511, Mar. 2020, doi: 10.1021/acssuschemeng.9b06635.

[14] L. Liu, M. Xu, Y. Ye, and B. Zhang, ‘On the degradation of (micro)plastics: Degradation methods, influencing factors, environmental impacts’, Feb. 01, 2022, *Elsevier B.V.* doi: 10.1016/j.scitotenv.2021.151312.

[15] S. Karbalaei, P. Hanachi, T. R. Walker, and M. Cole, ‘Occurrence, sources, human health impacts and mitigation of microplastic pollution’, Dec. 01, 2018, *Springer Verlag*. doi: 10.1007/s11356-018-3508-7.

[16] Z. Lin *et al.*, ‘Current progress on plastic/microplastic degradation: Fact influences and mechanism’, Jul. 01, 2022, *Elsevier Ltd*. doi: 10.1016/j.envpol.2022.119159.

[17] M. Edge *et al.*, ‘Aspects of Poly(ethylene terephthalate) Degradation for Archival Life and Environmental Degradation’, 1991.

[18] M. Niaounakis, *Additives for Polyolefins*. 2015.

[19] A. J. Peacock, *Handbook of Polyethylene: Structures, Properties and Applications.* New York: Marcel Dekker, 2000.

[20] J. D. Gu, ‘Microbiological deterioration and degradation of synthetic polymeric materials: Recent research advances’, *Int Biodeterior Biodegradation*, vol. 52, no. 2, pp. 69–91, 2003, doi: 10.1016/S0964-8305(02)00177-4.

[21] H. S. Auta, C. U. Emenike, B. Jayanthi, and S. H. Fauziah, ‘Growth kinetics and biodeterioration of polypropylene microplastics by Bacillus sp. and Rhodococcus sp. isolated from mangrove sediment’, *Mar Pollut Bull*, vol. 127, pp. 15–21, Feb. 2018, doi: 10.1016/j.marpolbul.2017.11.036.

[22] H. Alhazmi, F. H. Almansour, and Z. Aldhafeeri, ‘Plastic waste management: A review of existing life cycle assessment studies’, May 02, 2021, *MDPI AG*. doi: 10.3390/su13105340.

[23] A. Sherman, L. E. Hämmerle, E. Ben Mordechay, B. Chefetz, T. Hüffer, and T. Hofmann, ‘Uptake of tire-derived compounds in leafy vegetables

and implications for human dietary exposure', *Front Environ Sci*, vol. 12, May 2024, doi: 10.3389/fenvs.2024.1384506.

[24] S. Sridharan, M. Kumar, L. Singh, N. S. Bolan, and M. Saha, 'Microplastics as an emerging source of particulate air pollution: A critical review', Sep. 15, 2021, *Elsevier B.V.* doi: 10.1016/j.jhazmat.2021.126245.

[25] A. Siddiqua, J. N. Hahladakis, and W. A. K. A. Al-Attiya, 'An overview of the environmental pollution and health effects associated with waste landfilling and open dumping', Aug. 01, 2022, *Springer Science and Business Media Deutschland GmbH*. doi: 10.1007/s11356-022-21578-z.

[26] L. C. M. Lebreton, J. Van Der Zwet, J. W. Damsteeg, B. Slat, A. Andrady, and J. Reisser, 'River plastic emissions to the world's oceans', *Nat Commun*, vol. 8, Jun. 2017, doi: 10.1038/ncomms15611.

[27] L. Wilkie Johnston, E. Bergami, E. Rowlands, and C. Manno, 'Organic or junk food? Microplastic contamination in Antarctic krill and salps', *R Soc Open Sci*, vol. 10, no. 3, 2023, doi: 10.1098/rsos.221421.

[28] R. Geyer, J. R. Jambeck, and K. L. Law, 'Production, use, and fate of all plastics ever made', 2017. [Online]. Available: https://www.science.org

[29] R. Lehner, C. Weder, A. Petri-Fink, and B. Rothen-Rutishauser, 'Emergence of Nanoplastic in the Environment and Possible Impact on Human Health', Feb. 19, 2019, *American Chemical Society*. doi: 10.1021/acs.est.8b05512.

[30] M. Kazour, S. Terki, K. Rabhi, S. Jemaa, G. Khalaf, and R. Amara, 'Sources of microplastics pollution in the marine environment: Importance of wastewater treatment plant and coastal landfill', *Mar Pollut Bull*, vol. 146, pp. 608–618, Sep. 2019, doi: 10.1016/j.marpolbul.2019.06.066.

[31] S. Kihara, I. Köper, J. P. Mata, and D. J. McGillivray, 'Reviewing nanoplastic toxicology: It's an interface problem', Feb. 01, 2021, *Elsevier B.V.* doi: 10.1016/j.cis.2020.102337.

[32] S. L. Wright and F. J. Kelly, 'Plastic and Human Health: A Micro Issue?', *Environ Sci Technol*, vol. 51, no. 12, pp. 6634–6647, Jun. 2017, doi: 10.1021/acs.est.7b00423.

[33] E. Athanasopoulou, M. Tombrou, S. N. Pandis, and A. G. Russell, 'The role of sea-salt emissions and heterogeneous chemistry in the air quality

of polluted coastal areas', 2008. [Online]. Available: www.atmos-chem-phys.net/8/5755/2008/

[34] R. Dris, J. Gasperi, M. Saad, C. Mirande, and B. Tassin, 'Synthetic fibers in atmospheric fallout: A source of microplastics in the environment?', *Mar Pollut Bull*, vol. 104, no. 1–2, pp. 290–293, Mar. 2016, doi: 10.1016/j.marpolbul.2016.01.006.

[35] C. Cortés, J. Domenech, M. Salazar, S. Pastor, R. Marcos, and A. Hernández, 'Nanoplastics as a potential environmental health factor: Effects of polystyrene nanoparticles on human intestinal epithelial Caco-2 cells', *Environ Sci Nano*, vol. 7, no. 1, pp. 272–285, Jan. 2020, doi: 10.1039/c9en00523d.

[36] M. Cole, P. Lindeque, C. Halsband, and T. S. Galloway, 'Microplastics as contaminants in the marine environment: A review', Dec. 2011. doi: 10.1016/j.marpolbul.2011.09.025.

[37] H. Lee, W. J. Shim, and J. H. Kwon, 'Sorption capacity of plastic debris for hydrophobic organic chemicals', *Science of the Total Environment*, vol. 470–471, pp. 1545–1552, Feb. 2014, doi: 10.1016/j.scitotenv.2013.08.023.

[38] E. Colmenarejo Calero, M. Kovač Viršek, and N. Mali, 'Microplastics in Groundwater: Pathways, Occurrence, and Monitoring Challenges', May 01, 2024, *Multidisciplinary Digital Publishing Institute (MDPI)*. doi: 10.3390/w16091228.

[39] Y. L. Wang, Y. H. Lee, I. J. Chiu, Y. F. Lin, and H. W. Chiu, 'Potent impact of plastic nanomaterials and micromaterials on the food chain and human health', Mar. 01, 2020, *MDPI AG*. doi: 10.3390/ijms21051727.

[40] K. D. Cox, G. A. Covernton, H. L. Davies, J. F. Dower, F. Juanes, and S. E. Dudas, 'Human Consumption of Microplastics', *Environ Sci Technol*, vol. 53, no. 12, pp. 7068–7074, Jun. 2019, doi: 10.1021/acs.est.9b01517.

[41] A. M. I. Mowat, 'Anatomical basis of tolerance and immunity to intestinal antigens', 2003, *European Association for Cardio-Thoracic Surgery*. doi: 10.1038/nri1057.

[42] J. J. Powell, N. Faria, E. Thomas-McKay, and L. C. Pele, 'Origin and fate of dietary nanoparticles and microparticles in the gastrointestinal tract', *J Autoimmun*, vol. 34, no. 3, May 2010, doi: 10.1016/j.jaut.2009.11.006.

[43] A. H. Boag *et al.*, ‘The Pathology of Interstitial Lung Disease in Nylon Flock Workers’, *Am J Surg Pathol*, vol. 23, no. 12, 1999, [Online]. Available: https://journals.lww.com/ajsp/fulltext/1999/12000/the_pathology_of_interstitial_lung_disease_in.12.aspx

[44] V. Kopatz *et al.*, ‘Micro- and Nanoplastics Breach the Blood–Brain Barrier (BBB): Biomolecular Corona’s Role Revealed’, *Nanomaterials*, vol. 13, no. 8, Apr. 2023, doi: 10.3390/nano13081404.

[45] J. Hwang, D. Choi, S. Han, J. Choi, and J. Hong, ‘An assessment of the toxicity of polypropylene microplastics in human derived cells’, *Science of the Total Environment*, vol. 684, pp. 657–669, Sep. 2019, doi: 10.1016/j.scitotenv.2019.05.071.

[46] C. Bachert, ‘The role of histamine in allergic disease: Re-appraisal of its inflammatory potential’, 2002. doi: 10.1034/j.1398-9995.2002.1r3542.x.

[47] S. J. Galli, J. Kalesnikoff, M. A. Grimbaldeston, A. M. Piliponsky, C. M. M. Williams, and M. Tsai, ‘Mast cells as “tunable” effector and immunoregulatory cells: Recent advances’, 2005. doi: 10.1146/annurev.immunol.21.120601.141025.

[48] Q. Chen *et al.*, ‘Quantitative investigation of the mechanisms of microplastics and nanoplastics toward zebrafish larvae locomotor activity’, *Science of the Total Environment*, vol. 584–585, pp. 1022–1031, Apr. 2017, doi: 10.1016/j.scitotenv.2017.01.156.

[49] M. Schneider, F. Stracke, S. Hansen, and U. F. Schaefer, ‘Nanoparticles and their interactions with the dermal barrier’, *Dermatoendocrinol*, 2009.

[50] R. Alvarez-Román, A. Naik, Y. N. Kalia, R. H. Guy, and H. Fessi, ‘Skin penetration and distribution of polymeric nanoparticles’, *Journal of Controlled Release*, vol. 99, no. 1, pp. 53–62, Sep. 2004, doi: 10.1016/j.jconrel.2004.06.015.

[51] A. A. Koelmans, E. Besseling, and E. M. Foekema, ‘Leaching of plastic additives to marine organisms’, *Environmental Pollution*, vol. 187, pp. 49–54, Apr. 2014, doi: 10.1016/j.envpol.2013.12.013.

[52] K. Moriyama *et al.*, ‘Thyroid hormone action is disrupted by bisphenol A as an antagonist’, *Journal of Clinical Endocrinology and Metabolism*, vol. 87, no. 11, pp. 5185–5190, Nov. 2002, doi: 10.1210/jc.2002-020209.

[53] A. B. Ropero, P. Alonso-Magdalena, E. García-García, C. Ripoll, E. Fuentes, and A. Nadal, 'Bisphenol-A disruption of the endocrine pancreas and blood glucose homeostasis', in *International Journal of Andrology*, Blackwell Publishing Ltd, 2008, pp. 194–200. doi: 10.1111/j.1365-2605.2007.00832.x.

[54] C. G. Bornehag *et al.*, 'The association between asthma and allergic symptoms in children and phthalates in house dust: A nested case-control study', *Environ Health Perspect*, vol. 112, no. 14, pp. 1393–1397, Oct. 2004, doi: 10.1289/ehp.7187.

[55] Z. Cheng, X. P. Nie, H. S. Wang, and M. H. Wong, 'Risk assessments of human exposure to bioaccessible phthalate esters through market fish consumption', *Environ Int*, vol. 57–58, pp. 75–80, 2013, doi: 10.1016/j.envint.2013.04.005.

[56] D. Maestre-Batlle *et al.*, 'Dibutyl Phthalate Augments Allergen-induced Lung Function Decline and Alters Human Airway Immunology A Randomized Crossover Study', *Am J Respir Crit Care Med*, vol. 202, no. 5, pp. 672–680, Sep. 2020, doi: 10.1164/rccm.201911-2153OC.

[57] J. A. Bolaji *et al.*, 'Phthalates trigger respiratory reflexes', *European Respiratory Journal*, vol. 50, no. suppl 61, p. PA4785, Sep. 2017, doi: 10.1183/1393003.congress-2017.PA4785.

[58] A. Parthasarathy, A. C. Tyler, M. J. Hoffman, M. A. Savka, and A. O. Hudson, 'Is Plastic Pollution in Aquatic and Terrestrial Environments a Driver for the Transmission of Pathogens and the Evolution of Antibiotic Resistance?', Feb. 19, 2019, *American Chemical Society*. doi: 10.1021/acs.est.8b07287.

[59] S. Wagner *et al.*, 'First steps towards a generic sample preparation scheme for inorganic engineered nanoparticles in a complex matrix for detection, characterization, and quantification by asymmetric flow-field flow fractionation coupled to multi-angle light scattering and ICP-MS', *J Anal At Spectrom*, vol. 30, no. 6, pp. 1286–1296, Jun. 2015, doi: 10.1039/c4ja00471j.

[60] S. Kefer, O. Miesbauer, and H. C. Langowski, 'Environmental microplastic particles vs. Engineered plastic microparticles—a comparative review', Sep. 01, 2021, *MDPI*. doi: 10.3390/polym13172881.

[61] S. I. Hamdallah *et al.*, ‘Microfluidics for pharmaceutical nanoparticle fabrication: The truth and the myth’, *Int J Pharm*, vol. 584, Jun. 2020, doi: 10.1016/j.ijpharm.2020.119408.

[62] W. S. Lee, H. Kim, Y. Sim, T. Kang, and J. Jeong, ‘Fluorescent Polypropylene Nanoplastics for Studying Uptake, Biodistribution, and Excretion in Zebrafish Embryos’, *ACS Omega*, vol. 7, no. 2, pp. 2467–2473, Jan. 2022, doi: 10.1021/acsomega.1c06779.

[63] J. T. Jung, J. F. Kim, H. H. Wang, E. di Nicolo, E. Drioli, and Y. M. Lee, ‘Understanding the non-solvent induced phase separation (NIPS) effect during the fabrication of microporous PVDF membranes via thermally induced phase separation (TIPS)’, *J Memb Sci*, vol. 514, pp. 250–263, Sep. 2016, doi: 10.1016/j.memsci.2016.04.069.

[64] D. S. Achilias, A. Giannoulis, and G. Z. Papageorgiou, ‘Recycling of polymers from plastic packaging materials using the dissolution-reprecipitation technique’, *Polymer Bulletin*, vol. 63, no. 3, pp. 449–465, Sep. 2009, doi: 10.1007/s00289-009-0104-5.

[65] C. J. Martínez Rivas *et al.*, ‘Nanoprecipitation process: From encapsulation to drug delivery’, Oct. 30, 2017, *Elsevier B.V.* doi: 10.1016/j.ijpharm.2017.08.064.

[66] ‘IMPTOX’. Accessed: May 28, 2024. [Online]. Available: https://www.imptox.eu/en/

[67] D. S. Achilias, C. Roupakias, P. Megalokonomos, A. A. Lappas, and V. Antonakou, ‘Chemical recycling of plastic wastes made from polyethylene (LDPE and HDPE) and polypropylene (PP)’, *J Hazard Mater*, vol. 149, no. 3, pp. 536–542, Nov. 2007, doi: 10.1016/j.jhazmat.2007.06.076.

[68] S. J. Blott and K. Pye, ‘Particle size distribution analysis of sand-sized particles by laser diffraction: An experimental investigation of instrument sensitivity and the effects of particle shape’, *Sedimentology*, vol. 53, no. 3, pp. 671–685, Jun. 2006, doi: 10.1111/j.1365-3091.2006.00786.x.

I have tried to find all owners of the image rights and have obtained their permission to use the images in this thesis. Should a copyright infringement nevertheless become known, please contact me.

Appendix

Zusammenfassung

Die Umweltverschmutzung durch Plastik hat sich in den letzten Jahrzehnten zu einem wachsenden Problem entwickelt. Aufgrund ihrer hohen Stabilität und Persistenz haben Mikro- und Nanoplastik (MNPs) eine langsame Abbaurate und verbleiben mehrere Jahrzehnte in der Umwelt. Die Auswirkungen dieser MNPs auf das Ökosystem und die Gesundheit sind noch nicht vollständig erforscht, da ein erheblicher Mangel an verfügbaren Referenzmaterialien besteht. Daher ist die Entwicklung eines standardisierten Herstellungsverfahrens und eine umfassende Charakterisierung von Modellpartikeln aus Nanoplastik (NPs) erforderlich.

In der folgenden Arbeit wurde die Technik der nichtlösungsmittelinduzierten Phasentrennung (NIPS) zur Herstellung von Polyethylenterephthalat (PET) Nanopartikeln eingesetzt, da PET zu den weltweit meistverwendeten Polymeren in viele verschiedenen Anwendungsbereichen zählt. Ethanol (EtOH, 96%, v/v) wurde als Nichtlösungsmittel verwendet, während Benzylalkohol als Lösungsmittel diente. Die folgenden kritischen Parameter wurden identifiziert, die möglicherweise einen Einfluss auf die Partikelgrößenverteilung (PSD) der Modell-Nanopartikel haben: i) Rührzeit, ii) Filtrationszeit, iii) Zentrifugationszeit und iv) Zentrifugationsgeschwindigkeit. Die Optimierung dieser Parameter wurde dementsprechend untersucht. Für die Bestimmung der PSD wurde die Laser-Diffraktion (LD) eingesetzt. Nach der Optimierung wurde die Reproduzierbarkeit getestet, indem fünf aufeinanderfolgende Chargen mit dem optimierten Protokoll hergestellt wurden. Die Reproduzierbarkeit wurde durch die Mittelwerte der Perzentile (D10, D50 und D90), deren relativen Standardabweichungen (RSD), der Ausbeute (%) und dem Gleichmäßigkeitsfaktor bewertet. Das Ziel dieser Arbeit war es, Modell PET Nanopartikel, bei denen 85% der hergestellten Partikel kleiner als 1 µm sind, herzustellen. Weiters, wurden hinsichtlich der Reproduzierbarkeit RSDs von bis zu 15 % für D10, D50 und D90 toleriert.

Die Herstellung von PET NPs in EtOH (D10: 0,076 µm ± 0,0035 µm, D50: 0,172 µm ± 0,0056 µm, D90: 0,655 µm ± 0,3444 µm) und Glycerol (D10: 0,075 µm ± 0,0062 µm, D50: 0,172 µm ± 0,015 µm, D90: 0,462 µm ± 0,057 µm) führte zu

einer engen PSD und erreichte das Gesamtziel für alle Perzentile (n=5, Mittelwert ± Standardabweichung). Die RSDs (EtOH/Glycerol) von D10 (4,61%/8,30%) und D50 (3,27%/8,80%) konnten verbessert werden und erfüllten das gesetzte Kriterium. Die RSD von D90 in Glycerol erreichte ebenfalls das gesetzte Ziel (12,40%), während der Wert für Ethanol zu hoch war (52,57%). Mögliche Erklärungen sind die Bildung von Aggregaten und die Kontamination mit Staub während der Herstellung und Charakterisierung. Daher muss die Reproduzierbarkeit verbessert und in zukünftigen Studien weiter untersucht werden.